Bull. Soc. R. Sci. Liège, 2024, **93**(3), 85–102 *Peer-reviewed conference paper*
doi:10.25518/0037-9565.12274

An Interaction and Merger in a Massive Multiple System Create a Magnetic Field in a Massive Star

Abigail J. FROST[1,2,*], Hugues SANA[2], Laurent MAHY[3,2], Gregg WADE[4], James BARRON[5,4], Jean-Baptiste LE BOUQUIN[6], Antoine MÉRAND[7], Fabian R. N. SCHNEIDER[8,9], Tomer SHENAR[10,2], Rodolfo H. BARBÁ[11,†], Dominic M. BOWMAN[12,2], Matthias FABRY[13,2], Amin FARHANG[14], Pablo MARCHANT[2], Nidia I. MORRELL[15] and Jonathan V. SMOKER[1,16]

[1] European Southern Observatory, Alonso de Cordova 3107, Vitacura, Santiago, Chile
[2] Institute of Astronomy, KU Leuven, 3001 Leuven, Belgium
[3] Royal Observatory of Belgium, B–1180 Brussels, Belgium
[4] Department of Physics & Space Science, Royal Military College of Canada, Kingston Ontario K7K 0C6, Canada
[5] Department of Physics, Engineering & Astronomy, Queen's University, Kingston Ontario K7L 3N6, Canada
[6] Université Grenoble Alpes, Centre national de la recherche scientifique, Institut de Planétologie et d'Astrophysique de Grenoble, F–38000 Grenoble, France
[7] European Southern Observatory Headquarters, 85748 Garching bei München, Germany
[8] Heidelberger Institut für Theoretische Studien, 69118 Heidelberg, Germany
[9] Astronomisches Rechen-Institut, Zentrum für Astronomie der Universität Heidelberg, 69120 Heidelberg, Germany
[10] The School of Physics and Astronomy, Tel Aviv University, Tel Aviv, 69978, Israel
[11] Departamento de Física y Astronomía, Universidad de la Serena, La Serena, Chile
[12] School of Mathematics, Statistics and Physics, Newcastle University, Newcastle upon Tyne NE1 7RU, UK
[13] Villanova University, Dept. of Astrophysics and Planetary Science, 800 E Lancaster Ave, Villanova, PA 19085
[14] School of Astronomy, Institute for Research in Fundamental Sciences, 19395-5531 Tehran, Iran
[15] Las Campanas Observatory, Carnegie Observatories, La Serena, Chile
[16] UK Astronomy Technology Centre, Royal Observatory, Edinburgh EH9 3HJ, UK
[†] Deceased
[*] Corresponding author: abigail.frost@eso.org

Paper presented at the 41st Liège International Astrophysical Colloquium on "The eventful life of massive star multiples," University of Liège (Belgium), 15–19 July 2024.

Abstract

When stars are gravitationally bound in a binary or higher order multiple system there is a chance they can interact, enabling mass and momentum transfer. Such interactions can be life-changing events for the stars involved as they can change their internal mixing, final mass and

rotational speeds. In these proceedings, we describe our recent work which provides evidence that an interaction in a previous triple system caused a merger, the product of which is a magnetic star. This created the system as it is seen today – a massive binary system surrounded by an enriched ejecta nebula where only one of the massive stars is magnetic.

Keywords: stellar multiplicity, massive stars, magnetism

Résumé

Une interaction et une fusion dans un système multiple massif créent un champ magnétique dans une étoile massive. Dans un système binaire où les étoiles sont liées gravitationnellement, celles-ci peuvent interagir entre elles, entraînant un transfert de masse et de moment angulaire. De telles interactions ont un impact dramatique sur la vie des étoiles impliquées. En effet, ces interactions peuvent modifier leur masse finale, leurs vitesses de rotation ainsi que les processus de mélange à l'intérieur des étoiles mêmes. Ici, nous présentant les résultats nos travaux qui apportent, selon nous, la preuve qu'une interaction dans un système triple a provoqué la coalescence de la binaire centrale, résultant en une étoile magnétique. Cela a créé le système tel qu'il est vu aujourd'hui – un système binaire massif entouré d'une nébuleuse d'éjections enrichie où une seule des étoiles massives est magnétique.

Mots-clés : multiplicité stellaire, étoiles massives, magnétisme

1. Magnetism in Massive Stars

Magnetism is found throughout our Universe, including within the interiors of stars. Low-mass stars like the Sun harbour convective envelopes and the resultant cyclical movement of charged material throughout the Sun's envelope due to this convection sustains a dynamo effect which sustains the magnetic (B) field of our star. Such dynamo-induced B-fields can be found in many stars similar in mass to the Sun, creating B-fields of varying strengths. As stars become more massive however, the region of the stellar envelope that is convective shrinks with radiative heat transfer becoming more and more significant.

For the most massive stars of O spectral type the envelope is expected to be practically completely radiative. Despite this, $\sim 7\%$ of O stars show magnetic fields [1, 2], the origins of which are unclear. For stars that do host magnetic fields, the effect on their evolution can be significant. Harbouring a strong B field will limit stellar mass loss, as material which would otherwise be removed from the star due to its stellar winds is fed along field lines and back to the stellar equator. This can affect the type of core-collapse supernovae a massive star can go through [3] and lead to the formation of heavy-mass black holes (BH) [4]. Furthermore, they could create magnetars and cause long-duration gamma-ray bursts [5] and super-luminous supernovae [6].

A number of origins for magnetic fields in massive stars have been proposed. One possibility is that they could be remnant fields from the molecular clouds the stars formed from [7], that were compacted during the star formation process and sustained through convection during the

pre-main sequence phase [8]. However, it is difficult to explain why such fields would survive once the massive stars reached the main sequence, started to burn hydrogen and became mostly radiative [9].

Recently, theoretical models have shown that magnetic fields could be produced during a stellar interaction or merger [10]. Using 3D magnetohydrodynamical simulations for two merging main-sequence stars of ($9\,M_\odot$ and $8\,M_\odot$) and subsequent 1D stellar evolution modelling with MESA [11] illustrated this in the case of the massive magnetic star τ Sco [12]. Magneto-rotational instabilities induced in the merger product exponentially amplify the magnetic fields and the additional mixing of hydrogen in the merger product inspires further fusion, making the star appear younger than it is [13].

In the rest of this proceeding we will describe how a combination of observational techniques, launched by results found in spectro-interferometric data, allowed us to determine that the massive binary system HD 148937 may have gone through such a merger process to create just one magnetic star in the system [14].

The system studied is HD 148937 and is located at a position of RA (J2000): 16:33:52.387 and DEC (J2000): $-$48:06:40.476. The system has long been designated as an Of?p system due to the presence of strong C III and equally strong N III lines in its optical spectra [15], denoting chemical peculiarity. Additionally, variation has been noted in the Balmer emission of the system, with the width of the Hα line displaying short-period (7.03 d) variability [16–18] which some determined to be an indication of a magnetic field [19]. A dipolar magnetic field strength of 1020^{-380}_{+310} G was determined when the system was observed as part of the Magnetism in Massive Stars (MiMeS) survey [18]. As part of the Southern Massive Stars at High angular resolution survey, SMaSH, [20], the system was observed with the H-band interferometer PIONIER (the Precision Integrated-Optics Near-infrared Imaging ExpeRiment) [21] at the Very Large Telescope Interferometer (VLTI). The VLTI is a four-telescope interferometer that can either combine the beams of the four 8.2-m diameter Unit Telescopes (UTs) or the 1.8-m diameter Auxiliary Telescopes (ATs), with baselines ranging in length from about 40 to 200 m, providing milliarcsecond (mas) angular resolution measurements. Through this observation, the system was determined to be a binary composed of two stars of equal brightness in the H-band, with a separation between the two stars of 21.05 ± 0.67 mas. A multi-epoch spectral study of the system using around a decade's worth of spectra and the information from interferometry confirmed the system to be a double-lined spectroscopic binary [22]. Incomplete phase coverage and limited data quality within the spectra meant that a single orbital solution for the system could not be found, but reasonable solutions were possible for a period of 6617 ± 50 d and 9591 ± 350 d, with the latter being favoured.

2. Spectro-interferometric Data Launches a New Analysis of HD 148937

Interferometry is a powerful technique where an astronomical object is observed with multiple telescopes spread over large separations allowing us to view the source at higher angular resolution than with an individual telescope. The distance between the telescopes, or base-

lines, dictate the achieved resolution rather than the size of the primary mirror as is the case with imaging observations. The light retrieved at each telescope must be amalgamated to successfully probe the source, so interferometric observables are derived from coherence pattern of this light, or fringes, obtained through beam combination. Any interferometer provides the "visibility" – a measure of the spatial extent of the target. Visibility is a normalised quantity, and a visibility of 1 denotes a source that is unresolved by the interferometer (for example a distant star that appears as a point source), whilst visibilities lower than one show that the interferometer is spatially resolving the object. If the interferometer has at least three telescopes, the 'closure phase' is also obtained. This is the summation of three phases around a closed triangle of baselines (hence the need for three or more telescopes) and allows us to probe the symmetry of the source. If the closure phases are zero, the source is symmetric; if they deviate from zero, it is not. Through fitting models to interferometric observables we can determine the type of object/system that creates them. Geometric models using simple components formed of point sources, Gaussians, uniform discs and more can be sufficient for modelling stellar multiple systems.. Unresolved stars are easily modelled by uniform discs with diameters below the resolution limit of the interferometer for example. Fitting the visibility and closure phase alone can tell us how many stars are in a binary system, their flux ratio and their separations, with a resolution scale dictated by the baselines of the interferometer. In this way, interferometers provide a form of astrometric information, by accurately determining the positions of, say, the stars in a binary system. This is why the PIONIER datapoint of HD 148937 from [20] was used in the orbital analysis of [22].

Adding a spectrometer to an interferometer can push it to a new level of investigation. This is the case for the instrument GRAVITY at VLTI [23], which allows observations up to a spectral resolution $R \simeq 4000$. This means that in addition to the visibility and closure phases, GRAVITY also retrieves the "differential phase." This is essentially a measure of phase variations with wavelength. Fitting differential phases can be very powerful, as this phase variation provides angular information on objects on scales much smaller than the interferometer resolution limit [e.g., 24]. The normalised flux can also be fit when doing spectro-interferometry. If significant spectral lines are found, their effects will be visible in the differential phases and they can also potentially be resolved in the visibilities. The latter case is particularly exciting, as it means the region creating the line is being resolved. The new results we derive for HD 148937 could not have come to pass without spectro-interferometric data of the system. Two main epochs of VLTI/GRAVITY data were taken of the system with the ATs, with baselines of 49 to 129 m, corresponding to a maximum angular resolution of ~ 4 mas. An example of the interferometric data can be seen in Fig. 1. Two datasets are shown taken a couple of days apart. Subplot a) shows the u–v coverage of the observations – whereas points in image space can be described in terms of x and y, the points in Fourier space probed by the telescopes over the different baselines are described in terms of u and v. The baseline between each pair of telescopes possible in the interferometric array are shown in different colours, with the letters and numbers (e.g., J2) corresponding to the different positions of the telescopes [25]. We fit the data with geometric models using the code PMOIRED [26]. The model fits are in red, whilst the data are in black and errors in grey. Subplot b) shows the normalised flux with wavelength. Subplots c) to f)

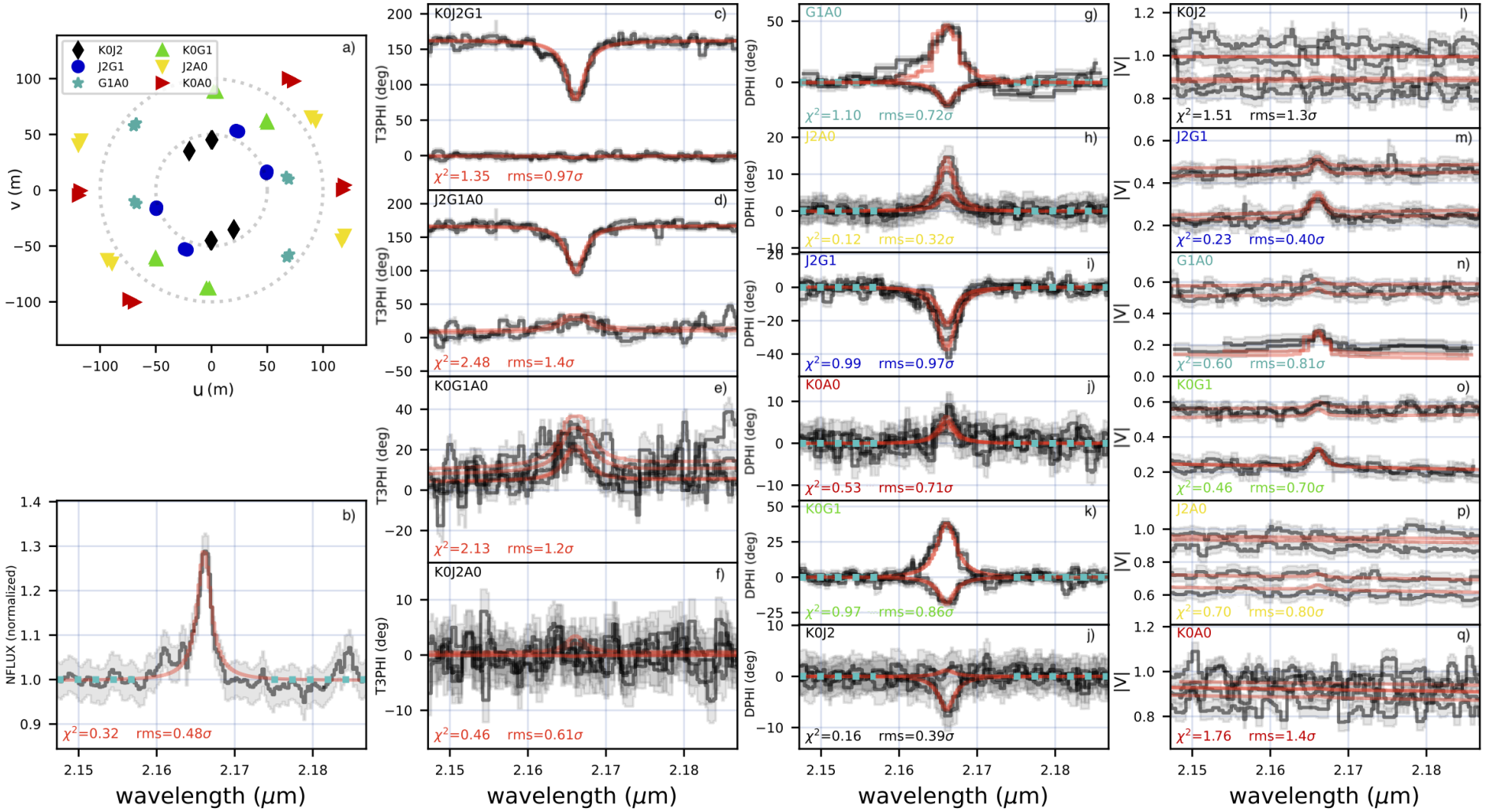

Figure 1: An example of the GRAVITY data of HD 148937.

are the closure phase measurements ("T3PHI") across different baselines, whilst subplots g) to j) are the differential phases ("DPHI") and subplots l) to q) are the visibilities $|V|$. The cyan squares represent the continuum which is computed using a linear fit. The text in each subplot is a different colour corresponding to the different baselines over which the measurement was taken (as in subplot a)).

To fit the data, we used the parametric modelling code PMOIRED [26]. PMOIRED allows the user not only to define geometrical components to represent stars and other astrophysical objects, but also lets you assign spectra and spectral line profiles to those components. This was crucial in our interpretation of the system, as a clear Br-γ emission line was visible in the normalised spectrum across all wavelengths and was slightly resolved in some baselines in the visibilities as well. The final model to the GRAVITY data confirmed the binary status of the system. The stars are of near equal brightness in the K-band, with the secondary being $\sim 95\%$ that of the primary on average. The key finding from the fitting process was that the best-fit was only obtained if a Lorentzian line profile to simulate the Br-γ emission was associated with *only* the primary star in the system. Given that we know the system as a whole harbours magnetism, this was somewhat surprising. Br-γ emission is an indirect sign of stellar winds confined by a magnetic field [e.g., 27], and is also used as a tracer of magnetospheres in hot stars [28–30]. Thus, our results from GRAVITY suggested that the primary star in HD 148937 was the only one to harbour the magnetic field. This is strange, given their similar luminosities (from the flux ratios). One could assume that the secondary and primary had become bound through dynamical interactions, but HD 148937 does not exist in a dense field or cluster environment necessary to make such a dynamical formation statistically likely. Also, since the stars look very similar, if the magnetic field was a remnant of the formation process, one would expect both of them to be magnetic, which the GRAVITY data implied not to be the case.

These results thus prompted us to revisit the system (and particularly its archival spectra) in more detail, to determine if other properties of the two stars in the binary also differed. In our analysis going forward, we assumed that, because the secondary did not show peculiarity according to our GRAVITY data, it was a typical O star and could be used as a reference to compare the properties of the magnetic star to.

3. Revisiting the Properties of the Binary System and its Stars

3.1. Orbit

The first step in our analysis was to better constrain the orbit. In addition to the aforementioned GRAVITY data, we also analysed more data from the PIONIER instrument. This resulted in an interferometric modelling over a period of ~ 9 yr. Given the lack of phase coverage of the archival optical spectra from [22] which were further confused by the presence of lines associated with chemical peculiarity and magnetism, we first attempted a fit solely with this astrometric data. The orbital fitting was done with the orbital solution finder spinOS [31] and Monte Carlo simulations were used to propagate the uncertainties on P, e, i and $M_{\rm total}$. We were able to converge on an astrometric-only fit, which pointed to a long-period (~ 29 yr), ec-

centric ($e = 0.77$) system in closer agreement with the longer period solution derived from [22]. From this fit, the derived total mass of the system of $56.52 \pm 0.75 M_{\odot}$ was incorporated into our further analysis. We then combined the astrometric dataset with the archival spectra and additional spectra from the Echelle SpectroPolarimetric Device for the Observation of Stars (ESPaDOnS) at the Canada France Hawaii Telescope (CFHT), using the final parameters from the astrometric-only fit as a first guess, providing our final orbital solution. With the constraint of the astrometric data, there was little difference between the astrometric-only fit and the combined data fit.

3.2. Spectral disentangling

Using the combined spectra we also used for the orbital fitting, we performed a spectral disentangling process to split the spectra for the whole system into a spectrum of the primary star and a spectrum of the secondary. Because HD 148937 shows spectral variability with $P = 7.03$ d [17, 18], a master spectrum was built at each epoch to remove these non-orbital variances. These master spectra were then used for the spectral disentangling process. Specifically a grid-disentangling approach [31–33] combined with a Fourier disentangling code [34] was used on spectral lines including He I+II λ4026 and He I λ4471. The semi-amplitudes of the RV curves (K_1 and K_2) were varied over a small grid, between 0 and 60 km s^{-1}, and the spectral signatures of each star separated without relying on previously measured RVs. To reduce the amount of degrees of freedom, most orbital parameters were fixed to those from interferometric fit.

K_2 was much harder to constrain than K_1 during the disentangling process. However, the total mass derived from the orbital fit to the interferometric data provided a way to better constrain it. The stellar masses of the individual stars in a binary can be related to their semi-amplitudes using Kepler's third law and the binary mass function [35]. Thus, since we had a total mass for the system, this essentially provided a region of semi-amplitudes that were possible for the system, given its calculated total mass. This region is illustrated in Fig. 2. Without this constraint, the solution for K_2 would have been ill-determined.

Because Fourier spectral disentangling has the disadvantage of losing the continuum when the system light curve does not have full eclipses, we also tried another separation technique, the shift-and-add method [36, 37]. The shift-and-add method yielded a 5 km s^{-1} difference between the K_2 values from the grid-disentangling method, which is not significant given the errors of both sets of values.

Finally, using our final K values and the total mass from interferometry we determined dynamical masses for each of the stars.

3.3. Atmospheric analysis

Once we had two spectra from the disentangling, atmospheric models from the CMFGEN stellar atmosphere code [38] were used to derive the properties of the stars corresponding to these spectral features. We chose to use the CMFGEN models because, again, the GRAVITY data and the solutions for individual spectra we derived implied that the secondary is essentially

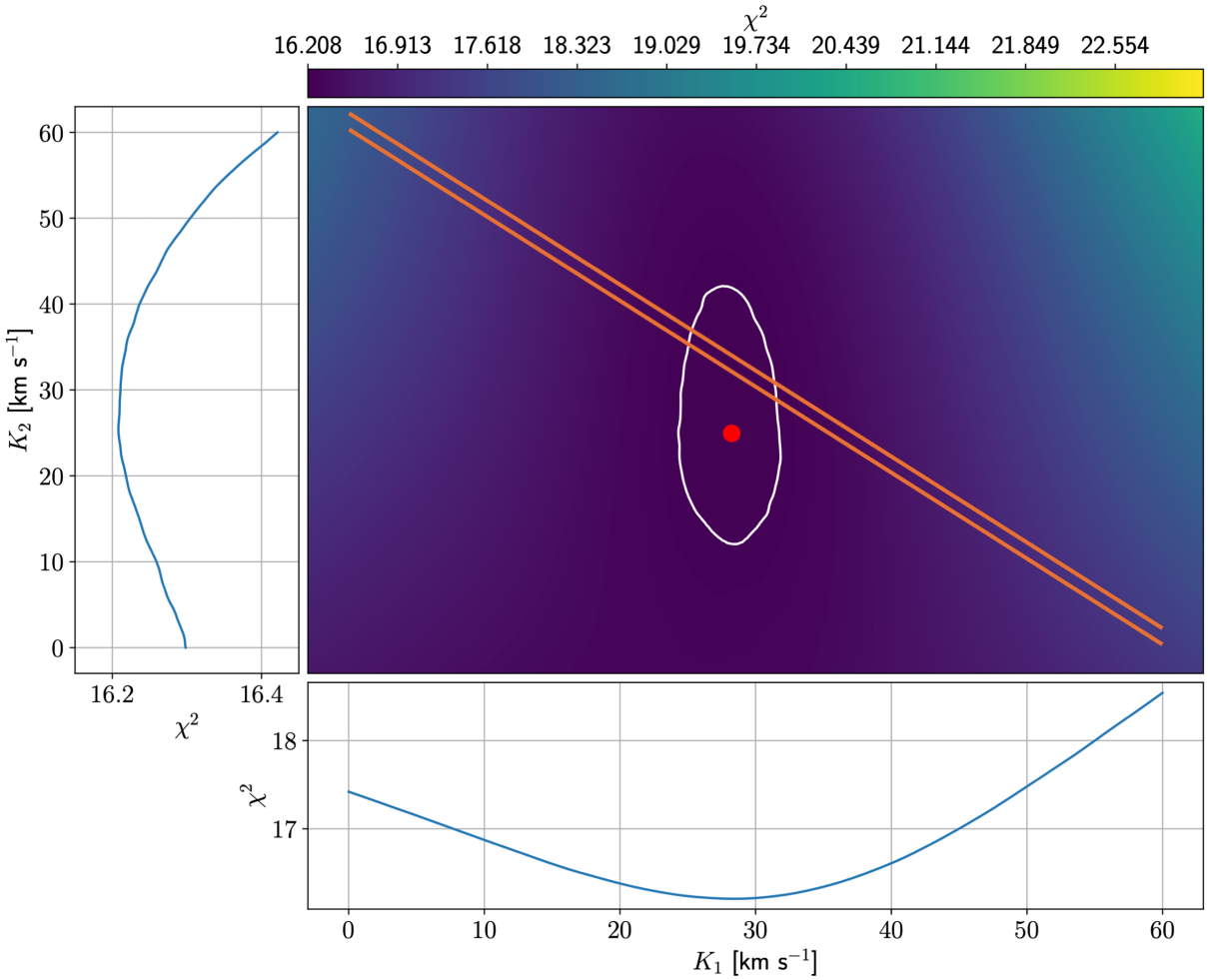

Figure 2: Reduced χ^2 map from the grid method of disentangling. The orange lines delimit the 68% confidence interval on the sum of the semi-amplitudes of both RV curves derived from the interferometric constraint on the total mass of the system. The minimal value at $K_1 = 28.4\,\mathrm{km\,s^{-1}}$ and $K_2 = 25.4\,\mathrm{km\,s^{-1}}$ is denoted with a red dot. The solid white contour is the 1σ level. The background gradient corresponds to the value of the χ^2 across the grid, with the colour-bar as reference. The side panels are 1D cut-through views of the axes of the χ^2 map.

Table 1: The parameters of the two stars in HD 148937 derived from our analysis with their 1σ confidence intervals. No value is derived for the nitrogen enrichment ($\varepsilon_{\rm N}$) for the primary star due to contamination from the lines associated with magnetism in this star. We denote this with the "..." symbol.

Parameter	Unit	Primary	Secondary
$T_{\rm eff}$	kK	$37.2^{+0.9}_{-0.4}$	$35.0^{+0.2}_{-0.9}$
$\log g$	cm s^{-2}	$4.00^{+0.09}_{-0.09}$	$3.61^{+0.05}_{-0.09}$
$v_{\rm eq} \sin i$	km s^{-1}	165 ± 20	67 ± 15
$v_{\rm macro}$	km s^{-1}	160 ± 38	78 ± 12
$f_i/f_{\rm tot}$	V-band	0.55 ± 0.02	0.45 ± 0.02
$\varepsilon_{\rm N}$	[log+12]	...	8.74 ± 0.10
$\log L/L_\odot$		5.28 ± 0.06	5.19 ± 0.07
M	$M_\odot$	$29.9^{+3.4}_{-3.1}$	$26.6^{+3.0}_{-3.4}$

a normal O-type star. The caveat with using the CMFGEN models is that they do not account for magnetic lines. As a result, there was no way to reproduce features such as the irregular Balmer lines, nor the C III or N III lines that allowed the system to be characterised as an Of?p system. In the fitting process to determine which CMFGEN models best reproduced the disentangled spectra of each star, these features were therefore not included in the chi-square minimisation. Ultimately solutions were found for both the primary and secondary. The main differences between the stars were their rotational velocities and the fact that, due to a lack of contamination due to the magnetic lines, we could determine that the secondary is likely nitrogen-enriched. Due to such contamination, any level of nitrogen enrichment could not be determined for the primary star.

3.4. Summary

The derived properties for each star are shown in Table 1. In the last two rows we also add the luminosities and masses of the stars. The luminosities were derived through SED fitting to the disentangled spectra and literature fluxes adjusted using the measured flux ratios of the two stars from interferometry. The masses were derived using the final values of the semi-amplitudes from the grid-disentangling and the total mass from the interferometric orbital fit.

With these properties, we plotted the two stars on a Hertzsprung–Russell diagram, shown in Fig. 3, where it is clear that the magnetic primary star appears younger than its secondary counterpart. To check our results, we used the BONNSAI grid of stellar evolution models [40] to determine if reasonable solutions that matched our final parameters could be found. They could, as the results also pointed towards an age difference – at least ~ 1.5 Myr in the case where nitrogen enrichment in the secondary was not considered, and ~ 4 Myr where it was. Therefore it appears that not only is the primary magnetic whilst the secondary is not, but

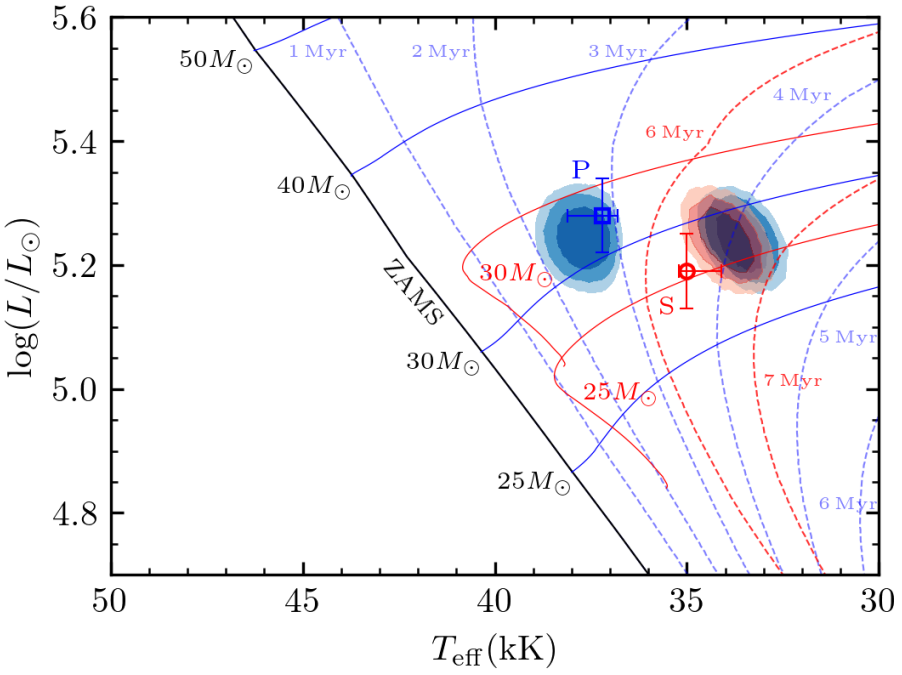

Figure 3: Hertzsprung–Russell diagram (HRD) illustrating the luminosities and temperatures of the primary (P) and secondary (S) based on our analysis (squares with error bars for 1σ confidence intervals). Coloured lines are isochrones and evolutionary tracks, with blue lines representing stars with an initial rotation of 165 km s^{-1}, whilst red lines represent stars with an initial rotation of 490 km s^{-1}. Dashed lines are isochrones for stellar populations with different ages. Solid lines are the evolutionary tracks for various initial masses computed at Galactic metallicity are those from [39]. The shaded contours show the 2D BONNSAI models which best fit the parameters we found. Blue applies to the primary and secondary in the case of no nitrogen enrichment while red applies to the secondary accounting for the nitrogen enrichment with 1, 2 and 3σ-confidence intervals.

assuming the secondary serves as an independent clock, the primary is also rejuvenated with respect to the secondary.

4. Our Theory for the Origin of HD 148937

To conclude, we describe our interpretation in the cause of the irregularities in the HD 148937 system. In order to create rejuvenation, a mechanism of mixing is required as the ignition of hydrogen makes the star appear brighter and therefore younger than it actually is. Mass-transfer through Roche Lobe OverFlow (RLOF) could cause rejuvenation of the primary magnetic star [e.g., 41, 42] as angular momentum gain could cause mixing and the rejuvenation of the accretor. However, from our analysis the secondary does not appear to be filling its Roche lobe and such events are also expected to circularise the orbit which is not seen. As mentioned

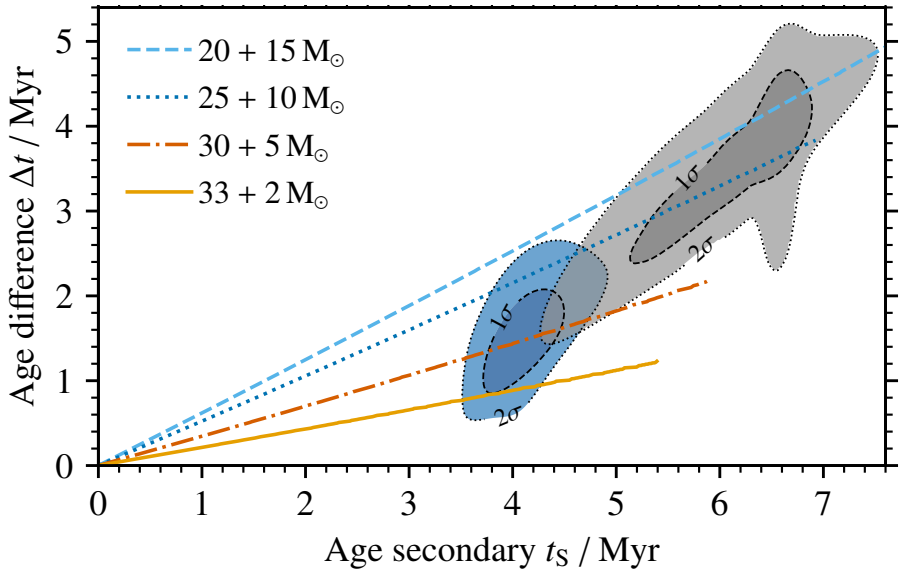

Figure 4: Merger and rejuvenation models compared to the measured properties of the HD 148937 system, with the age of the secondary star as a reference on the *x*-axis and the age difference between the rejuvenated primary and secondary shown on the *y*-axis. Each coloured/style of line shows a different model representing a scenario where two stars could have merged to form the current magnetic star in HD 148937. Shaded regions with contours are the observational constraints on the age of the secondary in the case where nitrogen enrichment is considered (grey) and the case where it is not (blue).

in the introduction though, modelling work has shown that mergers could also be responsible for the rejuvenation of massive stars *and* the generation of magnetic fields within them [12].

Another strange characteristic of the system is its surrounding nebula. Recent work with integral field spectra [43] derives a dynamical age of the nebula of just ~ 7500 yr. The nebula has various scales of structure, with clear bipolar lobes, a surrounding Strömgren sphere beyond this and more complex asymmetric structure within it [44]. The nebula is also enriched with CNO-process elements, with most enriched material in the most distant regions of the bipolar nebula [44]. Such enrichment is only expected within stellar interiors. Ejecta nebulae are also observed in the form of red novae for lower mass stars, some of which are thought to originate from stellar mergers [45, 46]. Furthermore, a chaotic merger of a triple system has been proposed as a formation mechanism for η Car and the Homunculus Nebula surrounding it [47].

In our interpretation of HD 148937 we decided to test whether a merger could explain the properties we find for the magnetic primary star. Using the same models as in the aforementioned analysis of τ Sco, we tried to find a solution that could explain the amount of rejuvenation we see between the primary and the secondary for HD 148937. Figure 4 shows the results. Using the secondary as a reference clock, we find several solutions that can reproduce the age of the secondary and the age difference between the primary and secondary. We use the ages

determined from the BONNSAI stellar evolution models and again consider two cases for the secondary, one where the nitrogen enrichment is considered and the case where it is not. 1-σ solutions exist in both cases, with the difference between the two manifesting in the mass ratio of the merger reactants. In the case where nitrogen enrichment is assumed to be present in the secondary (the smaller age discrepancy case), a more unequal mass merger of a $30_{\odot}$ and a $5M_{\odot}$ star provides a 1-σ solution, whilst if nitrogen enrichment is not considered and the age discrepancy is larger the merger of a $25M_{\odot}$ and a $10M_{\odot}$ star provides a 1-σ solution. In either case, the total mass required from the merged stars to produce the mass of the current magnetic primary star is $35M_{\odot}$. Therefore, between 1.7 and $8.2M_{\odot}$ would have to have been lost during the merger event. This nicely aligns which a previously estimated mass-range of the nebula of $1.6M_{\odot}$ to $12.6M_{\odot}$ [44] which, combined with the fact that it is enriched in stellar interior elements implies the ejecta nebula could have come from the merger as well.

Therefore, we conclude that the primary star in HD 148937 is likely the result of a merger event, which potentially created the surrounding nebula and caused HD 148937 to be a massive binary system with only one magnetic star. This implies that HD 148937 was likely originally a triple system, and the original tertiary star is the secondary star in the binary we see today. We invite the reader to consider our entire analysis in the form of the full paper [14].

Acknowledgments

Sadly our co-author Rodolfo Barbá passed away before our work was published. We offer our posthumous thanks for his enthusiasm for and contributions to this project.

Further Information

Authors' ORCID identifiers

0000-0001-9131-9970 (Abigail FROST)
0000-0001-6656-4130) (Hugues SANA)
0000-0003-0688-7987 (Laurent MAHY)
0000-0003-2088-0706 (James BARRON)
0000-0002-0493-4674 (Jean-Baptiste LE BOUQUIN)
0000-0003-2125-0183 (Antoine MÉRAND)
0000-0002-5965-1022 (Fabian SCHNEIDER)
0000-0003-0642-8107 (Tomer SHENAR)
0000-0001-7402-3852 (Dominic BOWMAN)
0000-0003-4200-7852 (Matthias FABRY)
0000-0001-7712-697X (Amin FARHANG)
0000-0002-0338-8181 (Pablo MARCHANT)
0000-0003-2535-3091 (Nidia MORRELL)
0000-0002-3082-7266 (Jonathan SMOKER)

Author contributions

AJF led the project, analysed the GRAVITY data, and wrote the original paper and these proceedings. HS co-led the project, prepared the observations of the PIONIER and GRAVITY data, calculated the absolute mass and luminosities and did the evolutionary modelling. AJF and HS did the orbital fitting. LM performed the spectral disentangling, atmospheric analysis and an independent estimate of the luminosities. GW organised the optical spectroscopic data and provided crucial insight into the previous spectroscopic analyses of the system. JB and DMB analysed the TESS data. JBLB reduced and analysed the PIONIER data. AM wrote the software used to analyse the GRAVITY data, reduced the GRAVITY data and assisted with its analysis. FRNS performed the merger modelling. TS discussed the results and cross-checked models. MF wrote the code for orbital fitting and assisted with the first attempts at the orbital fitting. RHB, AF, NIM and JVS observed the raw optical spectroscopic data. PM contributed to the theoretical interpretation. All co-authors contributed to the discussion and provided feedback during the manuscript preparation.

Conflicts of interest

We declare no conflict of interest.

References

[1] Wade, G. A., Neiner, C., Alecian, E., Grunhut, J. H., Petit, V., Batz, B. d., Bohlender, D. A., Cohen, D. H., Henrichs, H. F., Kochukhov, O., Landstreet, J. D., Manset, N., Martins, F., Mathis, S., Oksala, M. E., Owocki, S. P., Rivinius, T., Shultz, M. E., Sundqvist, J. O., Townsend, R. H. D., ud Doula, A., Bouret, J.-C., Braithwaite, J., Briquet, M., Carciofi, A. C., David-Uraz, A., Folsom, C. P., Fullerton, A. W., Leroy, B., Marcolino, W. L. F., Moffat, A. F. J., Nazé, Y., Louis, N. S., Aurière, M., Bagnulo, S., Bailey, J. D., Barbá, R. H., Blazère, A., Böhm, T., Catala, C., Donati, J.-F., Ferrario, L., Harrington, D., Howarth, I. D., Ignace, R., Kaper, L., Lüftinger, T., Prinja, R., Vink, J. S., Weiss, W. W., and Yakunin, I. (2016) The MiMeS survey of magnetism in massive stars: introduction and overview. *MNRAS*, **456**(1), 2–22. https://doi.org/10.1093/mnras/stv2568.

[2] Grunhut, J. H., Wade, G. A., Neiner, C., Oksala, M. E., Petit, V., Alecian, E., Bohlender, D. A., Bouret, J.-C., Henrichs, H. F., Hussain, G. A. J., Kochukhov, O., and the MiMeS Collaboration (2016) The MiMeS survey of Magnetism in Massive Stars: magnetic analysis of the O-type stars. *MNRAS*, **465**(2), 2432–2470. https://doi.org/10.1093/mnras/stw2743.

[3] Obergaulinger, M., Janka, H.-T., and Aloy, M. A. (2014) Magnetic field amplification and magnetically supported explosions of collapsing, non-rotating stellar cores. *MNRAS*, **445**(3), 3169–3199. https://doi.org/10.1093/mnras/stu1969.

[4] Petit, V., Keszthelyi, Z., MacInnis, R., Cohen, D. H., Townsend, R. H. D., Wade, G. A., Thomas, S. L., Owocki, S. P., Puls, J., and ud Doula, A. (2017) Magnetic massive stars

as progenitors of 'heavy' stellar-mass black holes. *MNRAS*, **466**(1), 1052–1060. https://doi.org/10.1093/mnras/stw3126.

[5] Bucciantini, N., Quataert, E., Metzger, B. D., Thompson, T. A., Arons, J., and Del Zanna, L. (2009) Magnetized relativistic jets and long-duration GRBs from magnetar spin-down during core-collapse supernovae. *MNRAS*, **396**(4), 2038–2050. https://doi.org/10.1111/j.1365-2966.2009.14940.x.

[6] Kasen, D. and Bildsten, L. (2010) Supernova light curves powered by young magnetars. *ApJ*, **717**(1), 245–249. https://doi.org/10.1088/0004-637X/717/1/245.

[7] Braithwaite, J. and Spruit, H. C. (2004) A fossil origin for the magnetic field in A stars and white dwarfs. *Natur*, **431**, 819–821. https://doi.org/10.1038/nature02934.

[8] Arlt, R. and Rüdiger, G. (2011) Amplification and stability of magnetic fields and dynamo effect in young Astars: Stability of magnetic fields in young A stars. *MNRAS*, **412**(1), 107–119. https://doi.org/10.1111/j.1365-2966.2010.17889.x.

[9] Moss, D. (2003) The survival of fossil magnetic fields during pre-main sequence evolution. *A&A*, **403**(2), 693–697. https://doi.org/10.1051/0004-6361:20030431.

[10] Ferrario, L., Pringle, J. E., Tout, C. A., and Wickramasinghe, D. T. (2009) The origin of magnetism on the upper main sequence. *MNRAS*, **400**(1), L71–L74. https://doi.org/10.1111/j.1745-3933.2009.00765.x.

[11] Paxton, B., Bildsten, L., Dotter, A., Herwig, F., Lesaffre, P., and Timmes, F. (2011) Modules for Experiments in Stellar Astrophysics (MESA). *ApJS*, **192**(1), 3. https://doi.org/10.1088/0067-0049/192/1/3.

[12] Schneider, F. R. N., Ohlmann, S. T., Podsiadlowski, Ph., Röpke, F. K., Balbus, S. A., Pakmor, R., and Springel, V. (2019) Stellar mergers as the origin of magnetic massive stars. *Natur*, **574**, 211–214. https://doi.org/10.1038/s41586-019-1621-5.

[13] Schneider, F. R. N., Podsiadlowski, Ph., Langer, N., Castro, N., and Fossati, L. (2016) Rejuvenation of stellar mergers and the origin of magnetic fields in massive stars. *MNRAS*, **457**(3), 2355–2365. https://doi.org/10.1093/mnras/stw148.

[14] Frost, A. J., Sana, H., Mahy, L., Wade, G., Barron, J., Le Bouquin, J.-B., Mérand, A., Schneider, F. R. N., Shenar, T., Barbá, R. H., Bowman, D. M., Fabry, M., Farhang, A., Marchant, P., Morrell, N. I., and Smoker, J. V. (2024) A magnetic massive star has experienced a stellar merger. *Sci*, **384**, 214–217. https://doi.org/10.1126/science.adg7700.

[15] Walborn, N. R. (1972) Spectral classification of OB stars in both hemispheres and the absolute magnitude calibration. *AJ*, **77**, 312–318. https://doi.org/10.1086/111285.

[16] Nazé, Y., Walborn, N. R., Rauw, G., Martins, F., Pollock, A. M. T., and Bond, H. E. (2008) HD 148937: A multiwavelength study of the third Galactic member of the Of?p class. *AJ*, **135**(5), 1946–1957. https://doi.org/10.1088/0004-6256/135/5/1946.

[17] Nazé, Y., ud Doula, A., Spano, M., Rauw, G., De Becker, M., and Walborn, N. R. (2010) New findings on the prototypical Of?p stars. *A&A*, **520**, A59. https://doi.org/10.1051/0004-6361/201014333.

[18] Wade, G. A., Grunhut, J., Gräfener, G., Howarth, I. D., Martins, F., Petit, V., Vink, J. S., Bagnulo, S., Folsom, C. P., Nazé, Y., Walborn, N. R., Townsend, R. H. D., and Evans, C. J. (2012) The spectral variability and magnetic field characteristics of the Of?p star HD 148937. *MNRAS*, **419**(3), 2459–2471. https://doi.org/10.1111/j.1365-2966.2011.19897.x.

[19] Hubrig, S., Schöller, M., Schnerr, R. S., González, J. F., Ignace, R., and Henrichs, H. F. (2008) Magnetic field measurements of O stars with FORS 1 at the VLT. *A&A*, **490**(2), 793–800. https://doi.org/10.1051/0004-6361:200810171.

[20] Sana, H., Le Bouquin, J.-B., Lacour, S., Berger, J.-P., Duvert, G., Gauchet, L., Norris, B., Olofsson, J., Pickel, D., Zins, G., Absil, O., de Koter, A., Kratter, K., Schnurr, O., and Zinnecker, H. (2014) Southern massive stars at high angular resolution: Observational campaign and companion detection. *ApJS*, **215**(1), 15. https://doi.org/10.1088/0067-0049/215/1/15.

[21] Le Bouquin, J.-B., Berger, J.-P., Lazareff, B., Zins, G., Haguenauer, P., Jocou, L., Kern, P., Millan-Gabet, R., Traub, W., Absil, O., Augereau, J.-C., Benisty, M., Blind, N., Bonfils, X., Bourget, P., Delboulbe, A., Feautrier, P., Germain, M., Gitton, P., Gillier, D., Kiekebusch, M., Kluska, J., Knudstrup, J., Labeye, P., Lizon, J.-L., Monin, J.-L., Magnard, Y., Malbet, F., Maurel, D., Ménard, F., Micallef, M., Michaud, L., Montagnier, G., Morel, S., Moulin, T., Perraut, K., Popovic, D., Rabou, P., Rochat, S., Rojas, C., Roussel, F., Roux, A., Stadler, E., Stefl, S., Tatulli, E., and Ventura, N. (2011) PIONIER: a 4-telescope visitor instrument at VLTI. *A&A*, **535**, A67. https://doi.org/10.1051/0004-6361/201117586.

[22] Wade, G. A., Smoker, J. V., Evans, C. J., Howarth, I. D., Barba, R., Cox, N. L. J., Morrell, N., Nazé, Y., Cami, J., Farhang, A., Walborn, N. R., Arias, J., and Gamen, R. (2019) A remarkable change of the spectrum of the magnetic Of?p star HD 148937 reveals evidence of an eccentric, high-mass binary. *MNRAS*, **483**(2), 2581–2591. https://doi.org/10.1093/mnras/sty3304.

[23] GRAVITY Collaboration: Abuter, R., Accardo, M., Amorim, A., Anugu, N., Ávila, G., Azouaoui, N., Benisty, M., Berger, J. P., Blind, N., Bonnet, H., and *123 more* (2017) First light for GRAVITY: Phase referencing optical interferometry for the Very Large Telescope ınterferometer. *A&A*, **602**, A94. https://doi.org/10.1051/0004-6361/201730838.

[24] Deshmukh, K., Sana, H., Mérand, A., Bodensteiner, J., Bordier, E., Dsilva, K., Frost, A. J., Gosset, E., Langer, N., Bouquin, J.-B. L., Lefever, R. R., Mahy, L., Patrick, L. R., Reggiani, M., Sander, A. A. C., Shenar, T., Tramper, F., Villaseñor, J. I., and Waisberg, I. (2024). Investigating 39 Galactic Wolf–Rayet stars with VLTI/GRAVITY: Uncovering a long period binary desert. arXiv e-prints: arXiv:2409.15212. https://doi.org/10.48550/arXiv.2409.15212.

[25] Haubois, X., Mérand, A., Abuter, R., Araneda, J. P., Bian, F., Bourget, P., Bristow, P., Burgos, P., Delplancke-Ströbele, F., Dembet, R., Gil, J. P., Glindemann, A., Gonté, F., Guajardo, P., Hubin, N., Hummel, C., Korhonen, H. H., Labdon, A., Kolb, J., Kosmalski, J., Lacour, S., Paladini, C., Pallanca, L., Pasquini, L., Percheron, I., Riquelme, M., Rivinius, T., Sani, E., Schmidtobreick, L., Scicluna, P., Schoeller, M., Schuhler, N., Tristram, K. R. W., Wittkowski, M., Woillez, J., and Zins, G. (2022) VLTI status update. In *Optical and Infrared Interferometry and Imaging VIII*, edited by Mérand, A., Sallum, S., and Sanchez-Bermudez, J., *SPIE Conference Series*, volume 12183. SPIE. https://doi.org/10.1117/12.2635405.

[26] Mérand, A. (2022) Flexible spectro–interferometric modeling of OIFITS data with PMOIRED. In *Optical and Infrared Interferometry and Imaging VIII*, edited by Mérand, A., Sallum, S., and Sanchez-Bermudez, J., *SPIE Conference Series*, volume 12183. SPIE. https://doi.org/10.1117/12.2626700.

[27] Ud-Doula, A., Owocki, S. P., and Townsend, R. H. D. (2008) Dynamical simulations of magnetically channelled line–driven stellar winds – II. The effects of field-aligned rotation. *MNRAS*, **385**(1), 97–108. https://doi.org/10.1111/j.1365-2966.2008.12840.x.

[28] Oksala, M. E., Grunhut, J. H., Kraus, M., Borges Fernandes, M., Neiner, C., Condori, C. A. H., Campagnolo, J. C. N., and Souza, T. B. (2015) An infrared diagnostic for magnetism in hot stars. *A&A*, **578**, A112. https://doi.org/10.1051/0004-6361/201525987.

[29] Wisniewski, J. P., Chojnowski, S. D., Davenport, J. R. A., Bartz, J., Pepper, J., Whelan, D. G., Eikenberry, S. S., Lomax, J. R., Majewski, S. R., Richardson, N. D., and Skrutskie, M. (2015) Characterizing the rigidly rotating magnetosphere stars HD 345439 and HD 23478. *ApJL*, **811**(2), L26. https://doi.org/10.1088/2041-8205/811/2/L26.

[30] Chojnowski, S. D., Hubrig, S., Labadie-Bartz, J., Rivinius, T., Schöller, M., Niemczura, E., Nidever, D. L., Stutz, A. M., and Hummel, C. A. (2022) Trumpler 16-26: a new centrifugal magnetosphere star discovered via SDSS/APOGEE *H*-band spectroscopy. *MNRAS*, **516**(2), 2812–2823. https://doi.org/10.1093/mnras/stac2396.

[31] Fabry, M., Hawcroft, C., Frost, A. J., Mahy, L., Marchant, P., Le Bouquin, J.-B., and Sana, H. (2021) Resolving the dynamical mass tension of the massive binary 9 Sagittarii. *A&A*, **651**, A119. https://doi.org/10.1051/0004-6361/202140452.

[32] Bodensteiner, J., Shenar, T., Mahy, L., Fabry, M., Marchant, P., Abdul-Masih, M., Banyard, G., Bowman, D. M., Dsilva, K., Frost, A. J., Hawcroft, C., Reggiani, M., and Sana, H. (2020) Is HR 6819 a triple system containing a black hole? An alternative explanation. *A&A*, **641**, A43. https://doi.org/10.1051/0004-6361/202038682.

[33] Shenar, T., Bodensteiner, J., Abdul-Masih, M., Fabry, M., Mahy, L., Marchant, P., Banyard, G., Bowman, D. M., Dsilva, K., Hawcroft, C., Reggiani, M., and Sana, H. (2020) The "hidden" companion in LB-1 unveiled by spectral disentangling. *A&A*, **639**, L6. https://doi.org/10.1051/0004-6361/202038275.

[34] Hadrava, P. (1995) Orbital elements of multiple spectroscopic stars. *A&AS*, **114**, 393–396. https://ui.adsabs.harvard.edu/abs/1995A&AS..114..393H.

[35] Remillard, R. A. and McClintock, J. E. (2006) X-ray properties of black-hole binaries. *ARA&A*, **44**, 49–92. https://doi.org/10.1146/annurev.astro.44.051905.092532.

[36] Marchenko, S. V., Moffat, A. F. J., and Eenens, P. R. J. (1998) The Wolf–Rayet binary WR 141 (WN5O + O5 V-III) revisited. *PASP*, **110**(754), 1416–1422. https://doi.org/10.1086/316280.

[37] González, J. F. and Levato, H. (2006) Separation of composite spectra: the spectroscopic detection of an eclipsing binary star. *A&A*, **448**(1), 283–292. https://doi.org/10.1051/0004-6361:20053177.

[38] Hillier, D. J. and Miller, D. L. (1998) The treatment of non-LTE line blanketing in spherically expanding outflows. *ApJ*, **496**(1), 407–427. https://doi.org/10.1086/305350.

[39] Brott, I., de Mink, S. E., Cantiello, M., Langer, N., de Koter, A., Evans, C. J., Hunter, I., Trundle, C., and Vink, J. S. (2011) Rotating massive main-sequence stars: I. Grids of evolutionary models and isochrones. *A&A*, **530**, A115. https://doi.org/10.1051/0004-6361/201016113.

[40] Schneider, F. R. N., Langer, N., de Koter, A., Brott, I., Izzard, R. G., and Lau, H. H. B. (2014) Bonnsai: a Bayesian tool for comparing stars with stellar evolution models. *A&A*, **570**, A66. https://doi.org/10.1051/0004-6361/201424286.

[41] Linder, N., Rauw, G., Martins, F., Sana, H., De Becker, M., and Gosset, E. (2008) High-resolution optical spectroscopy of Plaskett's star. *A&A*, **489**(2), 713–723. https://doi.org/10.1051/0004-6361:200810003.

[42] Grunhut, J. H., Wade, G. A., Leutenegger, M., Petit, V., Rauw, G., Neiner, C., Martins, F., Cohen, D. H., Gagne, M., Ignace, R., Mathis, S., de Mink, S. E., Moffat, A. F. J., Owocki, S., Shultz, M., Sundqvist, J., and the MiMeS Collaboration (2013) Discovery of a magnetic field in the rapidly rotating O-type secondary of the colliding-wind binary HD 47129 (Plaskett's star). *MNRAS*, **428**(2), 1686–1695. https://doi.org/10.1093/mnras/sts153.

[43] Lim, B., Nazé, Y., Chang, S.-J., and Hutsemékers, D. (2024) A morphokinematic study of the enigmatic emission nebula NGC 6164/5 surrounding the magnetic O-type star HD 148937. *ApJ*, **961**(1), 72. https://doi.org/10.3847/1538-4357/ad12c4.

[44] Mahy, L., Hutsemékers, D., Nazé, Y., Royer, P., Lebouteiller, V., and Waelkens, C. (2017) Evolutionary status of the Of?p star HD 148937 and of its surrounding nebula NGC 6164/5. *A&A*, **599**, A61. https://doi.org/10.1051/0004-6361/201629585.

[45] Pastorello, A., Mason, E., Taubenberger, S., Fraser, M., Cortini, G., Tomasella, L., Botticella, M. T., Elias-Rosa, N., Kotak, R., Smartt, S. J., Benetti, S., Cappellaro, E., Turatto,

M., Tartaglia, L., Djorgovski, S. G., Drake, A. J., Berton, M., Briganti, F., Brimacombe, J., Bufano, F., Cai, Y.-Z., Chen, S., Christensen, E. J., Ciabattari, F., Congiu, E., Dimai, A., Inserra, C., Kankare, E., Magill, L., Maguire, K., Martinelli, F., Morales-Garoffolo, A., Ochner, P., Pignata, G., Reguitti, A., Sollerman, J., Spiro, S., Terreran, G., and Wright, D. E. (2019) Luminous red novae: Stellar mergers or giant eruptions? *A&A*, **630**, A75. https://doi.org/10.1051/0004-6361/201935999.

[46] MacLeod, M., Ostriker, E. C., and Stone, J. M. (2018) Bound outflows, unbound ejecta, and the shaping of bipolar remnants during stellar coalescence. *ApJ*, **868**(2), 136. https://doi.org/10.3847/1538-4357/aae9eb.

[47] Hirai, R., Podsiadlowski, Ph., Owocki, S. P., Schneider, F. R. N., and Smith, N. (2021) Simulating the formation of η Carinae's surrounding nebula through unstable triple evolution and stellar merger-induced eruption. *MNRAS*, **503**(3), 4276–4296. https://doi.org/10.1093/mnras/stab571.